



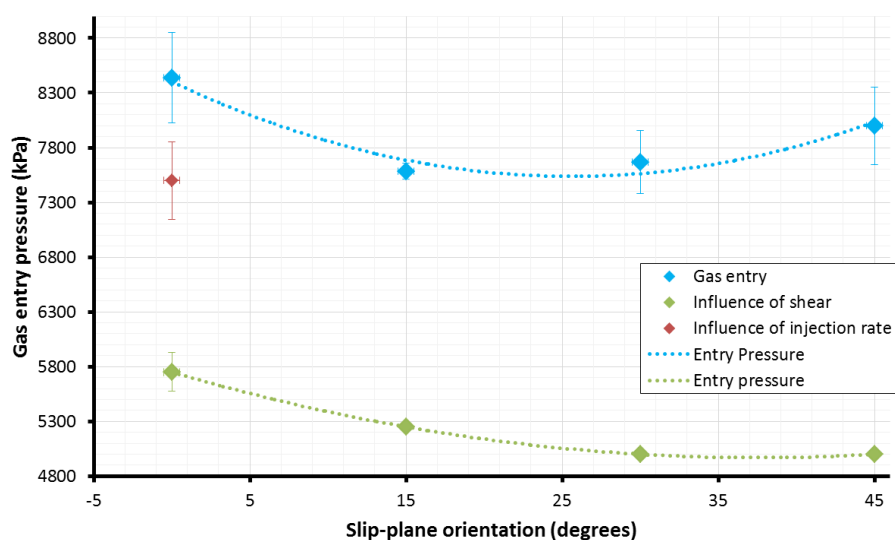
**British
Geological Survey**

NATURAL ENVIRONMENT RESEARCH COUNCIL

Summary Report of FORGE WP4.1.2: Verification of critical stress theory applied to repository concepts

Minerals and Waste Programme

Commissioned Report CR/12/146



BRITISH GEOLOGICAL SURVEY

MINERALS AND WASTE PROGRAMME

COMMISSIONED REPORT CR/12/146

Summary Report of FORGE WP4.1.2: Verification of critical stress theory applied to repository concepts

R.J. Cuss, J.F. Harrington, S. Sathar, and H.J. Reeves

Keywords

Critical stress theory, fracture transmissivity, fracture flow, kaolinite, shear testing.

Front cover

Gas entry pressure for all tests showing the influence of gas injection rate, active shear, and feature orientation. This plot validates the critical stress theory

Bibliographical reference

CUSS, R.J., HARRINGTON, J.F., SATHAR, S., and REEVES, H.J. 2012. Summary Report of FORGE WP4.1.2: Verification of critical stress theory applied to repository concepts. *British Geological Survey Commissioned Report*, CR/12/146. 27pp.

Copyright in materials derived from the British Geological Survey's work is owned by the Natural Environment Research Council (NERC) and/or the authority that commissioned the work. You may not copy or adapt this publication without first obtaining permission. Contact the BGS Intellectual Property Rights Section, British Geological Survey, Keyworth, e-mail ipr@bgs.ac.uk. You may quote extracts of a reasonable length without prior permission, provided a full acknowledgement is given of the source of the extract.

BRITISH GEOLOGICAL SURVEY

The full range of our publications is available from BGS shops at Nottingham, Edinburgh, London and Cardiff (Welsh publications only) see contact details below or shop online at www.geologyshop.com

The London Information Office also maintains a reference collection of BGS publications, including maps, for consultation.

We publish an annual catalogue of our maps and other publications; this catalogue is available online or from any of the BGS shops.

The British Geological Survey carries out the geological survey of Great Britain and Northern Ireland (the latter as an agency service for the government of Northern Ireland), and of the surrounding continental shelf, as well as basic research projects. It also undertakes programmes of technical aid in geology in developing countries.

The British Geological Survey is a component body of the Natural Environment Research Council.

British Geological Survey offices

BGS Central Enquiries Desk

Tel 0115 936 3143 Fax 0115 936 3276

email enquires@bgs.ac.uk

Kingsley Dunham Centre, Keyworth, Nottingham NG12 5GG

Tel 0115 936 3241 Fax 0115 936 3488

email sales@bgs.ac.uk

Murchison House, West Mains Road, Edinburgh EH9 3LA

Tel 0131 667 1000 Fax 0131 668 2683

email scotsales@bgs.ac.uk

London Information Office at the Natural History Museum (Earth Galleries), Exhibition Road, South Kensington, London SW7 2DE

Tel 020 7589 4090 Fax 020 7584 8270

Tel 020 7942 5344/45 email bgs london@bgs.ac.uk

Columbus House, Greenmeadow Springs, Tongwynlais, Cardiff CF15 7NE

Tel 029 2052 1962 Fax 029 2052 1963

Forde House, Park Five Business Centre, Harrier Way, Sowton EX2 7HU

Tel 01392 445271 Fax 01392 445371

Maclean Building, Crowmarsh Gifford, Wallingford OX10 8BB

Tel 01491 838800 Fax 01491 692345

Geological Survey of Northern Ireland, Colby House, Stranmillis Court, Belfast BT9 5BF

Tel 028 9038 8462 Fax 028 9038 8461

www.bgs.ac.uk/gsni/

Parent Body

Natural Environment Research Council, Polaris House, North Star Avenue, Swindon SN2 1EU

Tel 01793 411500 Fax 01793 411501

www.nerc.ac.uk

Website www.bgs.ac.uk

Shop online at www.geologyshop.com

Foreword

This report is the product of a study by the British Geological Survey (BGS) undertaken on behalf of the Nuclear Decommissioning Authority – Radioactive Waste Management Directorate (NDA-RWMD) and the European Union 7th Framework Euratom Programme under the auspices of the Fate of repository Gases (FORGE) project, to examine the validation of critical stress theory applied to repository concept and the influence of fracture/fault angle on gas flow properties. This report represents the contribution to the Work Package 4 summary report. The full experimental report is given in Cuss *et al.*, 2013.

Acknowledgements

The study was undertaken by staff of the Minerals and Waste Programme of the BGS using the experimental facilities of the Transport Properties Research Laboratory (TPRL). Funding for the study was provided by the Nuclear Decommissioning Authority – Radioactive Waste Management Directorate (NDA-RWMD), the European Union (FORGE Project) and the British Geological Survey through its well-founded laboratory programme. The authors would like to thank the skilled staff of the Research & Development Workshops at the BGS, in particular Humphrey Wallis, for their design and construction of the experimental apparatus.

Contents

| | |
|--|-----------|
| Foreword | 2 |
| Acknowledgements | 2 |
| Contents | 3 |
| Executive summary | 5 |
| 1 Introduction | 6 |
| 1.1 Rationale | 6 |
| 1.2 Objectives | 7 |
| 2 Experimental set-up | 8 |
| 3 Results | 9 |
| 3.1 Loading-unloading tests..... | 10 |
| 3.2 Gas breakthrough experiments | 16 |
| 3.3 General observations | 21 |
| 4 Conclusions | 22 |
| References | 23 |

FIGURES

| | |
|---|----|
| Figure 1-1 - Critical stress hypothesis..... | 7 |
| Figure 2-1 – Schematic of the Angled Shear Rig (ASR). | 8 |
| Figure 3-1 – Example of hysteresis seen in water flow during a loading/unloading experiment on a 30° slip-plane. | 10 |
| Figure 3-2 – Example of loading-unloading cycle seen during a gas injection tests on a 30° slip-plane..... | 11 |
| Figure 3-3 – Fracture width recorded during a loading-unloading experiment. | 12 |
| Figure 3-4 – Shear displacement caused as the result of loading-unloading. | 12 |
| Figure 3-5 – The hysteresis observed in horizontal stress during loading-unloading experiments | 13 |
| Figure 3-6 – The variation of the ratio of horizontal stress to vertical stress seen during loading-unloading experiments..... | 14 |
| Figure 3-7 – Comparing results for water and gas injection during loading and unloading experiments | 15 |
| Figure 3-8 – Results from ASR_Tau06_30gGI showing different gas breakthrough indicating fault-valve behaviour | 17 |
| Figure 3-9 – Repeatability of gas injection tests; a) pressure response, b) flow results. | 18 |
| Figure 3-10 – Gas injection pressure variation with discontinuity orientation. | 19 |
| Figure 3-11 – Comparing gas entry pressure with normal load on the fracture..... | 19 |

Figure 3-12 – Gas injection pressure variation with discontinuity orientation and the influence of shear and injection rate. 20

Figure 3-13 – The influence of gas pressurisation rate. 20

Figure 3-14 – Photo showing the escape of gas into from the slip-plane. 21

Figure 3-15 – Example of pressure recorded on the slip-plane..... 22

Executive summary

This report outlines the major conclusions from an experimental study of 48 separate experiments with the primary aim to verify critical stress theory. Two main types of experiment were conducted: 1). Loading-unloading tests, where fracture flow was monitored at constant injection pressure as normal load was increased in steps to a given level and then reduced back to the starting stress state; 2). Gas breakthrough experiments, where gas injection pressure was increased in a pressure ramp at constant vertical load. These were conducted with and without active shear. It was found that critical stress theory is valid in predicting the preferential flow of gas in relation to the orientation of the fracture plane with respect to the maximum horizontal stress direction. However, loading unloading experiments showed that understanding the stress history of the rocks is of paramount importance and a mere knowledge of the current stress state is insufficient in accurately predicting the nature of fluid flow.

1 Introduction

1.1 RATIONALE

Discontinuities (fracture, faults, joints, interfaces, etc) play a pivotal role in controlling the movement of water and gas around an underground disposal facility (GDF) for radioactive waste. According to the current concepts, high level and long lived radioactive waste and spent fuel are intended to be stored/disposed of in a GDF within a stable geological formations (host rock) at depth (usually ~50-800 meters) beneath the ground surface. Hence, the radioactive waste is securely isolated and contained. At depth the rock mass may be a naturally fractured environment, such is the case for a GDF in crystalline rock, and the excavation of the GDF galleries is recognised to induce additional fractures (Bossart *et al.*, 2002; Rutqvist *et al.*, 2009). Therefore, all current concepts of disposal, be these in argillaceous, crystalline or salt rocks, will have a multitude of discontinuities as part of the engineered environment within the EDZ. Depending on the *in situ* stress conditions, preferential pathways may form along any, or all, of these discontinuities.

Fluids, such as gases and water, are expected to play a role in the transport of radionuclides away from the GDF. The conductivity of fluids through discontinuities is understood to be controlled by the interplay of their orientation and stress tensor direction (Barton *et al.*, 1995; Finkbeiner *et al.*, 1997). Around the GDF there are two distinct zones with differing discontinuity orientation, discontinuity densities, and fluid flow properties; (a) the EDZ where an intricate range of discontinuity (fracture) orientations are present in a complex localised-stress field, and (b) the far field zone where discontinuous (pre-fractured/faulted) host rock may be present.

It has been proposed that discontinuities that are oriented parallel to the maximum horizontal stress orientation (σ_H) experience the lowest normal stresses acting across them and therefore will undergo the least amount of closure and will thus be the most permeable (Heffer & Lean, 1993). This is based on the assumption that discontinuities experiencing the least amount of stress will offer minimum resistance to flow and therefore will have relatively high permeability. However, observations by Laubach *et al.* (2004) on a number of sedimentary basins in the western United States using core permeability, stress measurements, and fluid flow datasets showed that at a depth of >3 km, the open discontinuities were not aligned parallel to σ_H as previously understood. Hence, *in situ* stress orientations cannot be realistically used as an indicator for predicting fluid flow in fractured rocks.

Barton *et al.* (1995) proposed that discontinuities whose state of stress are close to the failure criterion are more likely to be conductive because of the localised failure as a consequence of the large shear component acting along the discontinuity surface. Such features are termed “critically stressed” and are oriented approximately 30 degrees to σ_H (Rogers, 2003; Rogers & Evans, 2002). In order to apply the critical stress theory to the study of flow, the *in situ* stress field acting along all discontinuities in a volume of rock can be resolved into shear and normal stress components. When the magnitude and direction of the stress field has been constrained, the shear stress (τ) and normal stress (σ_n) acting on a discontinuity can be expressed by (Jaeger *et al.*, 2007):

$$\tau = \beta_{11}\beta_{21}\sigma_1 + \beta_{12}\beta_{22}\sigma_2 + \beta_{13}\beta_{23}\sigma_3 \quad \text{and} \quad \sigma_n = \beta_{11}^2\sigma_1 + \beta_{12}^2\sigma_2 + \beta_{13}^2\sigma_3$$

where, β_{ij} = directional cosines between the discontinuity and the stress tensor, σ_1 , σ_2 , and σ_3 = magnitude of the maximum, intermediate, and minimum principal stresses respectively.

When the shear stress and normal stress on the discontinuities are plotted with respect to the *in situ* stress field in a Mohr space, the faults and fractures that are scattered above the Mohr-Coulomb failure criterion are termed critically stressed and hence expected to be conductive

(Figure 1-1). Critically stressed discontinuities are expected to be present amongst the numerous complex fracture networks within and around the EDZ and in the far field around the GDF.

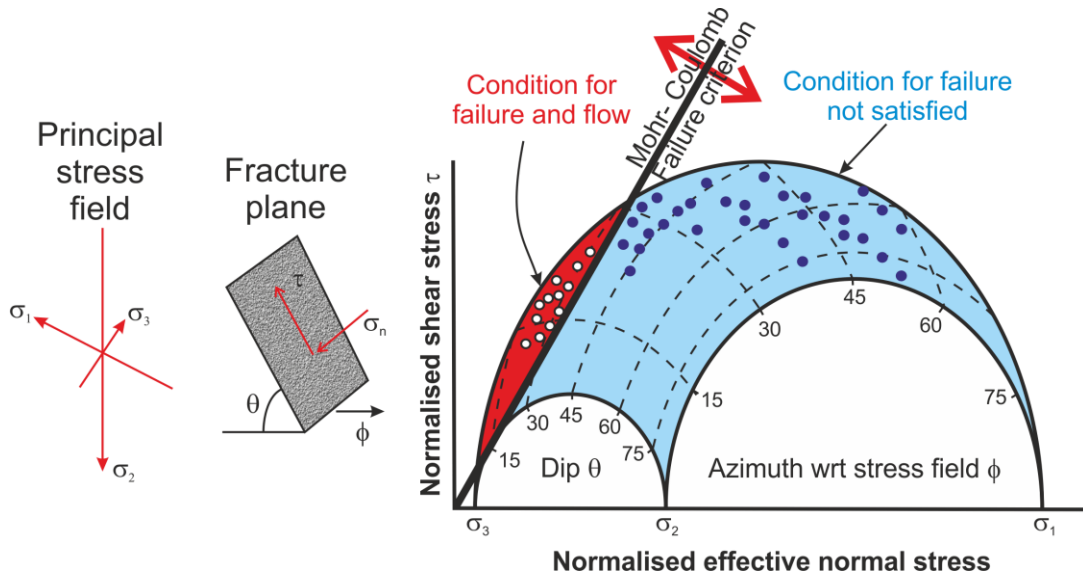


Figure 1-1 - Critical stress hypothesis (adopted from Barton *et al.*, 1995; Jaeger *et al.*, 2007; Rogers, 2003). The three-dimensional Mohr diagram represents the shear stress and normal stress acting along a fracture in response to the *in situ* stress field. The open circles represent fractures experiencing state of stress above the failure criterion and therefore subject to shear failure. The closed circles represent fractures whose stress state is insufficient to induce shear failure and hence stable.

1.2 OBJECTIVES

Whilst there is considerable field evidence for the applicability of the critical stress approach from many sedimentary basins worldwide, the theory has been found to be lacking in describing the flow regime in the Sellafield area, UK (Reeves 2002). This previous research explained the discrepancy by considering the tectonic history of the region. Sellafield has undergone uplift and the stress acting on the faulted bedrock is now lower than at the time of their formation. Therefore, this study showed that the flow regime of discontinuities is more complex than the simple critical state approach would predict.

The objective of this experimental programme was to examine the relationship between the stress tensor direction and discontinuity orientation, as well as examining the conditions under which discontinuities become conductive. In doing this experimentation it will validate the critical stress theory, which could be used to understand the reasons why some fractures in the EDZ are conductive and hence aid performance assessment. Specific objectives were:

- (i) perform and interpret small scale experiments to investigate relationship between the stress tensor direction and fracture orientations, as well as examining the conditions under which fractures become conductive,
- (ii) provide high-quality experimental data to test/validate the critical stress theory in relation to repository condition for the first time.

Previous work at BGS on fracture transmissivity in Opalinus clay (Cuss *et al.*, 2011) designed an effective apparatus and showed that flow is a complex, focused, transient property that is dependent upon normal stress, shear displacement, fracture topology, fluid composition, and swelling characteristics of the material. The current experimental programme aimed to extend this knowledge by investigating the influence of discontinuity orientation. The programme was not proscribed and investigation of other factors influencing flow were explored. However, some

elements of discontinuity flow were only “identified” and will require follow-up work in order to describe fully their influence.

2 Experimental set-up

All experiments were performed using the bespoke Angled Shear Rig (ASR, Figure 2-1) designed and built at the British Geological Survey. Experiments conducted on Opalinus clay (Cuss *et al.*, 2011) have shown that fracture topology is a key parameter in controlling fluid flow along fractures. In order to reduce the number of variables required to fully understand discontinuity flow, a “generic” discontinuity was investigated. The ASR comprised of two stainless steel blocks with a clay gouge of saturated kaolinite (gravimetric water content of 80%) of 60mm × 60 mm × 50 μm sandwiched between them. This allows the pure mechanical influence of discontinuity orientation to be investigated in a simplified system. Results are also applicable to clay-rich and crystalline disposal concepts in the numerous discontinuities seen.

The ASR comprised 6 main components:

1. Rigid frame that has been designed to deform as little as possible during the experiment;
2. Vertical load system comprising an Enerpac hydraulic ram that is controlled using an ISCO 260D syringe pump, a rigid loading frame and an upper thrust block (up to 20 MPa normal stress, 72 kN force);
3. Shear force actuator designed to drive shear as slow as 14 microns a day at a constant rate (equivalent to 1 mm in 69 days);
4. Pore pressure system comprising an ISCO 500D syringe pump that can deliver either water or gas through the centre of the top block directly to the fracture surface;
5. A state-of-the-art custom designed data acquisition system using National Instruments LabVIEW™ software facilitating the remote monitoring and control of all experimental parameters.
6. The experimental slip plane assembly consisting of precision machined 316 stainless steel top and bottom blocks with dips of 0, 15, 30, and 45 degrees forming fault plane. The top block was connected to the vertical loading mechanism by means of a swivel mechanism which was engaged to the shoulders on either side of the top block.

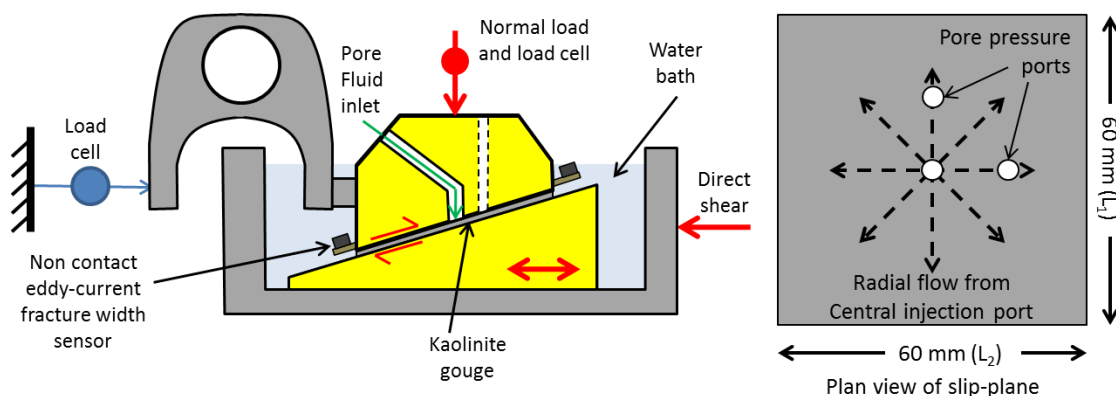


Figure 2-1 – Schematic of the Angled Shear Rig (ASR).

Unlike standard direct shear experiments, the top and bottom blocks could be oriented at different angles to the vertical load/horizontal displacement. Experiments were conducted on horizontal blocks and angles of 0, 15, 30, and 45 degrees. Vertical load was applied using a servo controlled Teledyne ISCO-260D syringe pump pressurising an Enerpac single acting hydraulic ram connected to a rigid loading frame. The Enerpac ram had a stroke of 105 mm, which meant

that the ram could easily accommodate the vertical displacement of the top block as it rode up the fracture surface at constant vertical load. Pore fluid (water or helium) was introduced through the centre of the top block by means of a Teledyne ISCO 500D syringe pump connected in series to a gas-water interface vessel. Pore pressure transducers, attached to ports which were positioned orthogonally to each other at 15 mm from the central pore fluid inlet allowed measurement of pore pressures within the slip plane (see Figure 2-1). The shear-force actuator was comprised of an ISCO 500 series D syringe pump, which was modified by mounting horizontally. The ISCO pump was designed to push a syringe through a barrel to deliver pressure. In the current setup, the barrel had been removed and the drive-train directly connected to the sample assembly, itself mounted on a low friction bearing. Horizontal load was measured using a load cell fitted laterally to the top-block.

The upper and lower thrust blocks of the apparatus were made out of stainless steel with a contact area of 60 mm × 60 mm. The lower thrust block was longer than the top one so that the contact area was maintained constant throughout the test. Vertical travel of the thrust block (giving gouge dilation) was measured by a high precision non-contact capacitance displacement transducer, which had a full range of ± 0.5 mm and an accuracy of 0.06 µm. Following early testing, it was necessary to add two high precision Eddy current non-contact displacement transducers to either end of the top thrust block in order to record gouge thickness directly and to determine non-parallel alignment of the two thrust blocks. These submersible devices had a full range of ± 1 mm and an accuracy of 0.2 µm. Lateral movement was measured using a high precision linear variable differential transformer (LVDT), which had a full range of ± 25 mm and an accuracy of 0.5 µm

3 Results

The complete experimental programme conducted 48 separate experiments. All experimental results are described in Cuss *et al.* (2013). Two main types of experiment were conducted: 1). Loading-unloading tests, where fracture flow was monitored at constant injection pressure as vertical load was increased in steps to a given level and then reduced back to the starting stress state; 2). Gas breakthrough experiments, where gas injection pressure was increased in a pressure ramp at constant vertical load. These were conducted with and without active shear. In addition, a number of other experiments were conducted. The main conclusions from this study are summarised below:

3.1 Loading-unloading tests:

- 3.1.1 During a loading (vertical stress) and unloading cycle considerable hysteresis in flow was observed signifying the importance of stress history on fracture flow.
- 3.1.2 For the case of gas injection the change in flow was chaotic at low vertical loads, whereas for water injection the flow reduced smoothly with increased vertical load.
- 3.1.3 Hysteresis in horizontal stress observed during unloading demonstrated the importance of the ratio between horizontal stress and vertical stress and its control on flow.
- 3.1.4 Differences have been observed between injection fluids (water and helium), especially the hysteresis observed in flow. For water injection flow was only partially recovered during unloading, whereas for gas enhanced flow was seen at low vertical loads.

3.2 Gas breakthrough experiments:

- 3.2.1 During gas breakthrough experiments episodic flow/fault valve behaviour was seen with a decrease in subsequent peak pressures and the form of the pressure response was different during subsequent breakthrough events.

- 3.2.2 Repeat gas injection testing has shown a consistent gas entry pressure but considerably different, non-repeatable, gas peak pressures.
- 3.2.3 Differences in gas entry pressure were seen dependent on the orientation of the fracture.
- 3.2.4 Active shear reduced the gas entry pressure, which is contrary to observations seen in Opalinus clay.

3.3 General observations:

- 3.3.1 The results showed that the flow of gas through clay filled fractures was non-uniform and occurred via localised preferential pathways.
- 3.3.2 The pressure recorded within the slip-plane showed a negligible fracture pressure and did not vary much in all tests.

Each finding is discussed in more detail below.

3.1 LOADING-UNLOADING TESTS

A total of 17 loading-unloading experiments were conducted, all on a 30° slip-plane. Nine tests were conducted without a permeant in order to understand the behaviour of the kaolinite gouge whilst loading/unloading, five tests were conducted with water as the injection fluid, whilst three gas flow experiments were conducted.

3.1.1 During a loading (vertical stress) and unloading cycle considerable hysteresis in flow was observed signifying the importance of stress history on fracture flow.

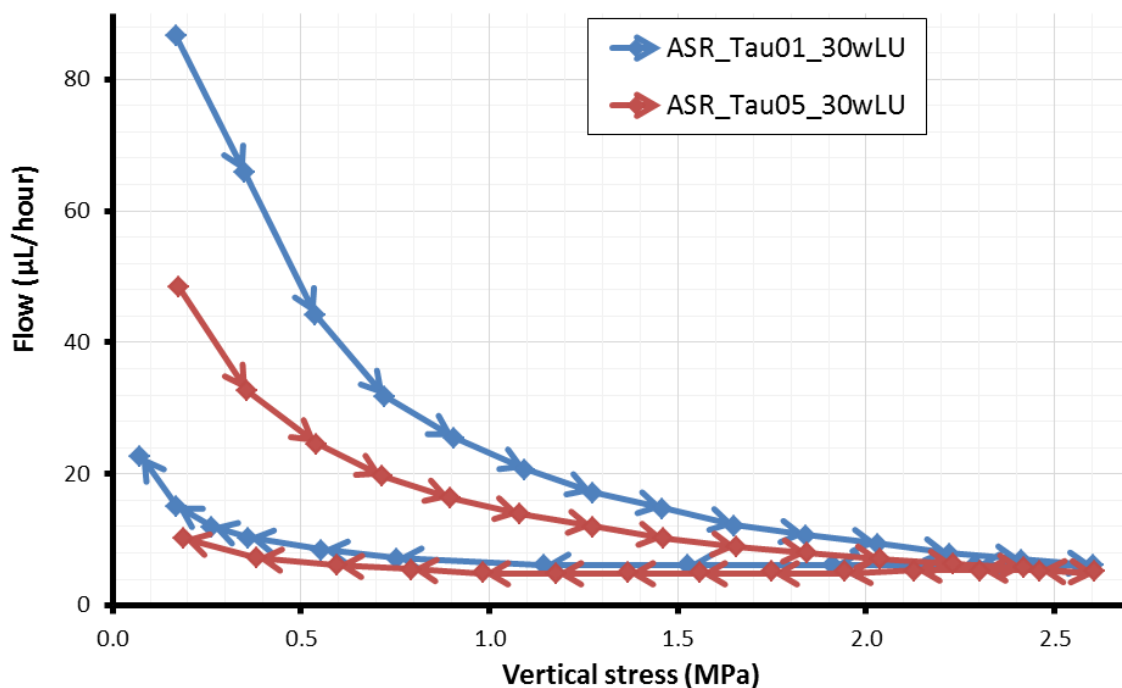


Figure 3-1 – Example of hysteresis seen in water flow during a loading/unloading experiment on a 30° slip-plane.

Figure 3-1 shows the results of flow achieved for two tests conducted injecting water into a 30° discontinuity during loading from 0.1 to 2.6 MPa and unloading from 2.6 to 0.2 MPa. As can be seen, the starting flow rate of the two tests were different by nearly a factor of 5. Both tests were setup in identical ways using the same pre-mixed weight of kaolinite and deionised water. This difference may have derived from variations of gouge thickness and as a result the experimental system was modified in order to measure the starting gouge thickness.

As normal load was increased in steps, the flow along the slip plane steadily reduced. In both experiments, although starting from dissimilar flow rates, both achieved a flow rate of approximately 6 $\mu\text{L/h}$ by 2.6 MPa vertical load. On unloading, this flowrate did not significantly alter until vertical loads of approximately 0.75 MPa. Therefore it can be noted that the “memory” of the maximum load experienced was retained. This illustrates the importance of stress history on predicting flow along discontinuities and has been used to explain the non-applicability of the critical stress approach in its simple form at the Sellafield site in the UK (Sathar *et al.*, 2012).

All loading-unloading experiments showed marked hysteresis in flow.

3.1.2 For the case of gas injection the change in flow was chaotic at low vertical loads, whereas for water injection the flow reduced smoothly with increased vertical load.

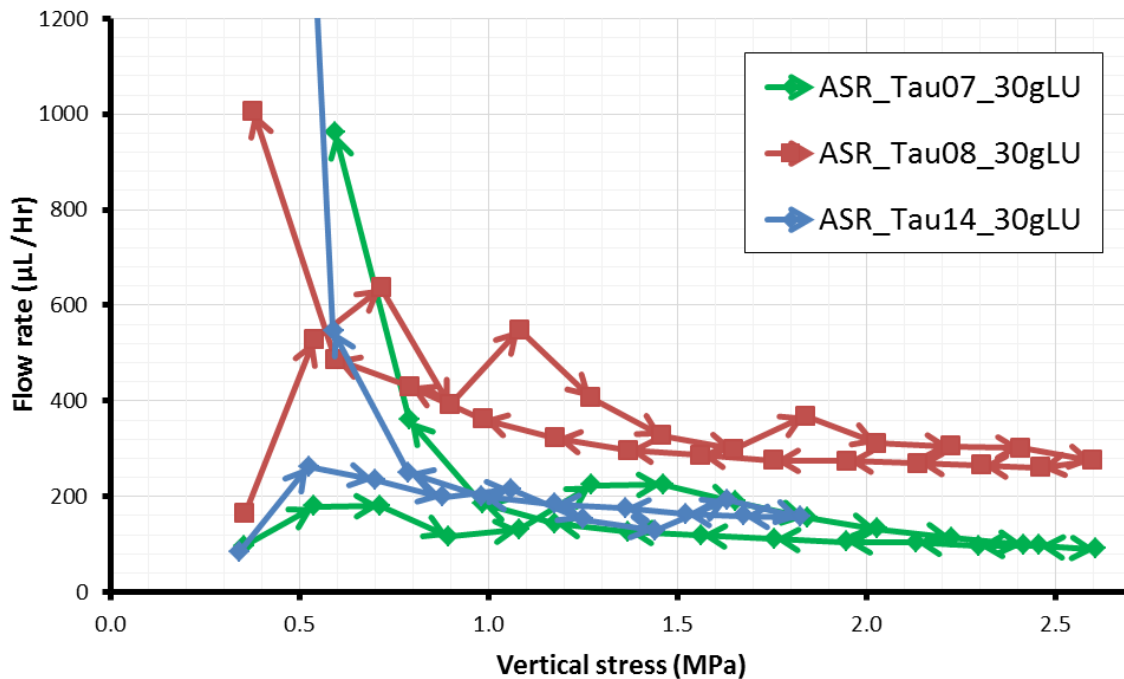


Figure 3-2 – Example of loading-unloading cycle seen during a gas injection tests on a 30° slip-plane.

Figure 3-2 shows the results for three loading-unloading experiments with gas as the injection medium. Considerable differences are seen between the loading and unloading cycles. On loading the progression of flow was chaotic. In all three tests, once vertical load was increased from the starting value of approximately 0.3 to 0.5 MPa flow increased. All three tests showed that increased vertical load resulted in episodes of increasing and decreasing flow. This could be explained by 3 possible mechanisms:

1. Gas flow was highly sensitive to water content of the gouge and the duration of the experiment meant that full drainage was not possible;
2. The gouge was not remaining even in thickness along the complete length, i.e. increased load was resulting in a wedge shaped gouge;
3. Shear movement was occurring along the 30° slope as vertical load was increased and there was some form of stick-slip, which meant that the movement was uneven between steps.

It is difficult to rule out scenario (1) as this had not been investigated fully. However, wide variation in flow rates have not been observed, which suggests that a fairly homogenous paste of gouge had been created and that subtle, localised changes in saturation (caused by uneven drainage) was unlikely to be the main cause of this effect.

The second scenario (2) is not supported by the measurement of the gouge thickness during experimentation, as seen in Figure 3-3. Even reduction in gouge thickness was observed, with

more chaotic variations in thickness seen during unloading. This is contrary to the flow data, where chaotic flow was seen during loading and even variation seen during unloading. Therefore this effect was unlikely to be caused by uneven thicknesses of gouge.

The third scenario (3) is also not supported by experimental observations. Figure 3-4 shows that there was shear movement as a result of only increasing vertical load. However, this increased relatively evenly and suggests that changes in load have resulted in the gouge moving evenly.

Observations of localised flow suggests that gas exploits sub-micronscale features within the clay, similar to features observed in bentonite. The exact cause of the chaotic behaviour has not been determined due to the macro-scale of measurement and the likely microscopic origin of this behaviour. However, the chaotic behaviour was repeatable and suggests that gas flow predictions of transmissivity are problematic. The “even” reduction in flow on unloading supports the “memory” effect of the clay introduced in the previous section.

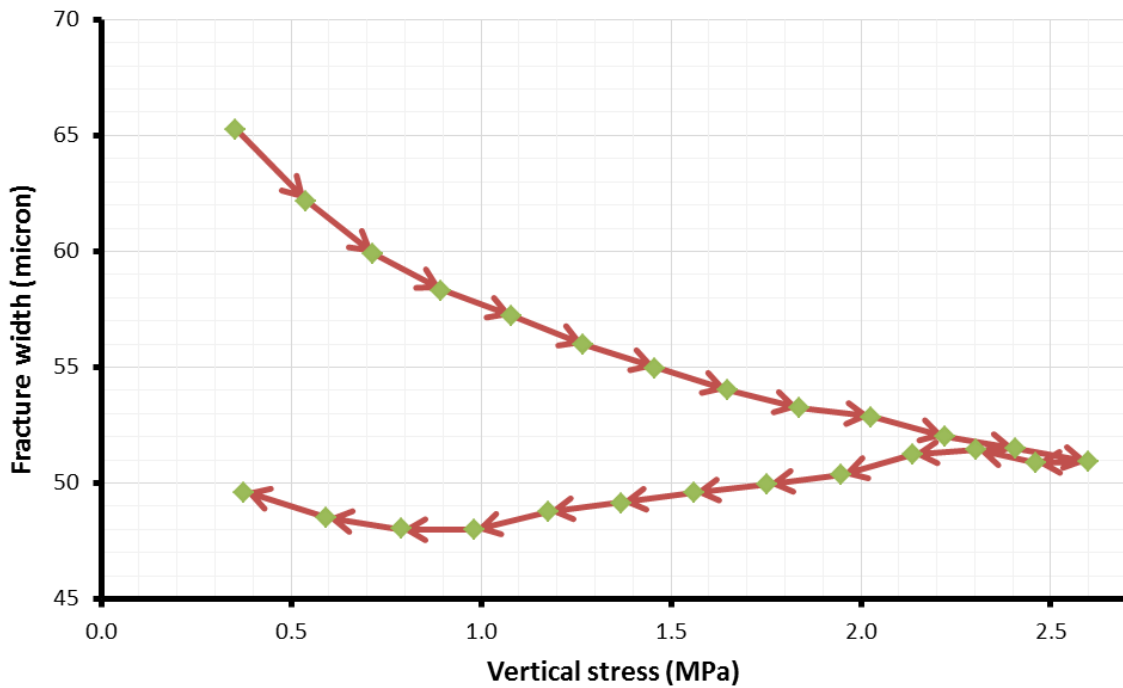


Figure 3-3 – Fracture width recorded during a loading-unloading experiment.

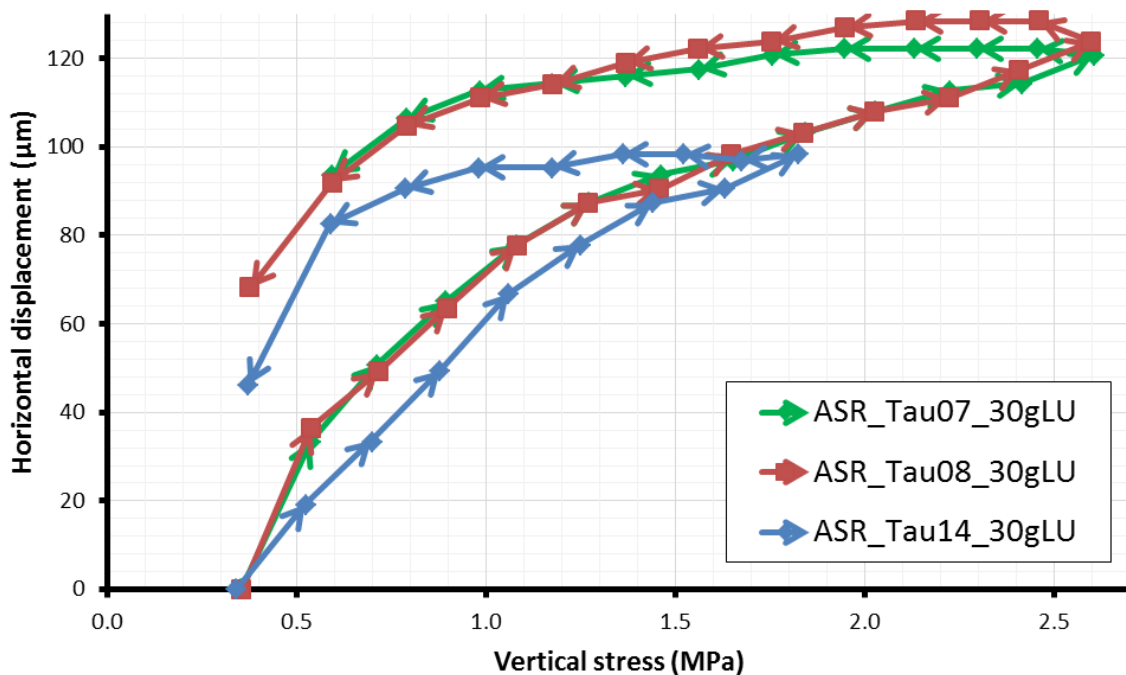


Figure 3-4 – Shear displacement caused as the result of loading-unloading.

3.1.3 Hysteresis in horizontal stress observed during unloading demonstrates the importance of the ratio between horizontal stress and vertical stress and its control on flow.

Figure 3-5 shows that considerable hysteresis was observed in horizontal stress during loading-unloading experiments for both water and gas injection. The repeatability of the results showed that free movement of the gouge was achieved. The hysteresis in horizontal stress during unloading may be attributed to the cohesive strength of the kaolinite clay gouge. Figure 3-6 shows how the ratio of horizontal stress to vertical stress varied during the experiment. Here, subtle variation between water and gas injection experiments was seen during unloading once the ratio exceeded unity. Significant gas flow rate increase occurred when the horizontal stress to vertical stress ratio increased above unity during unloading.

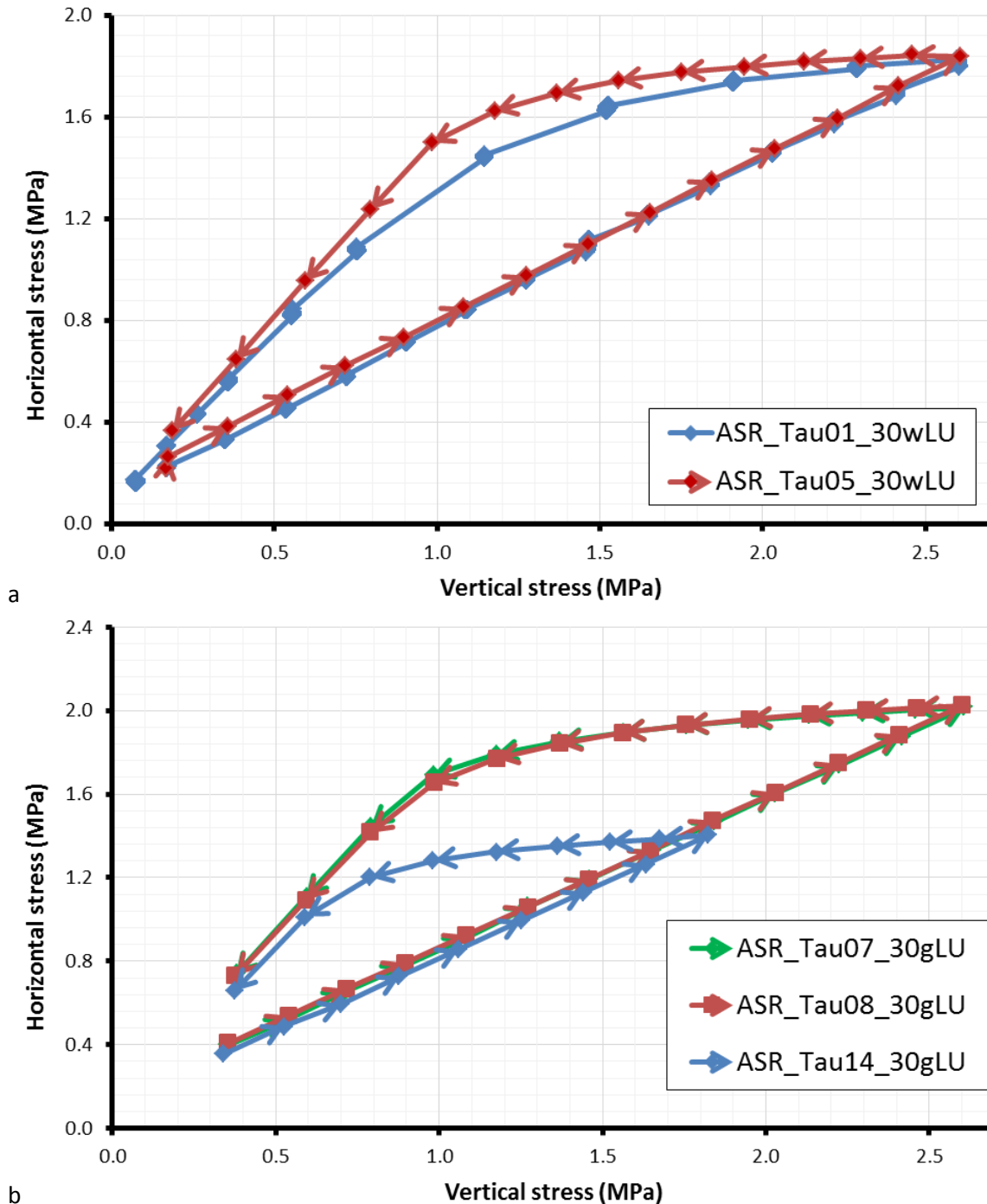


Figure 3-5 – The hysteresis observed in horizontal stress during loading-unloading experiments; a) water injection; b) gas injection.

Zoback *et al.* (1985) and Brudy *et al.* (1997) have shown that the ratio of shear stress to normal stress is crucial in controlling permeability and in the movement of gas through fractures. The close relationship between fracture flow and the horizontal to vertical stress ratio during the unloading stages in the present experiments also points towards its significance in understanding the flow of fluid through discontinuities. In the case of a fractured rock formation undergoing uplift stress relaxation is likely to result in a high horizontal stress to vertical stress ratio.

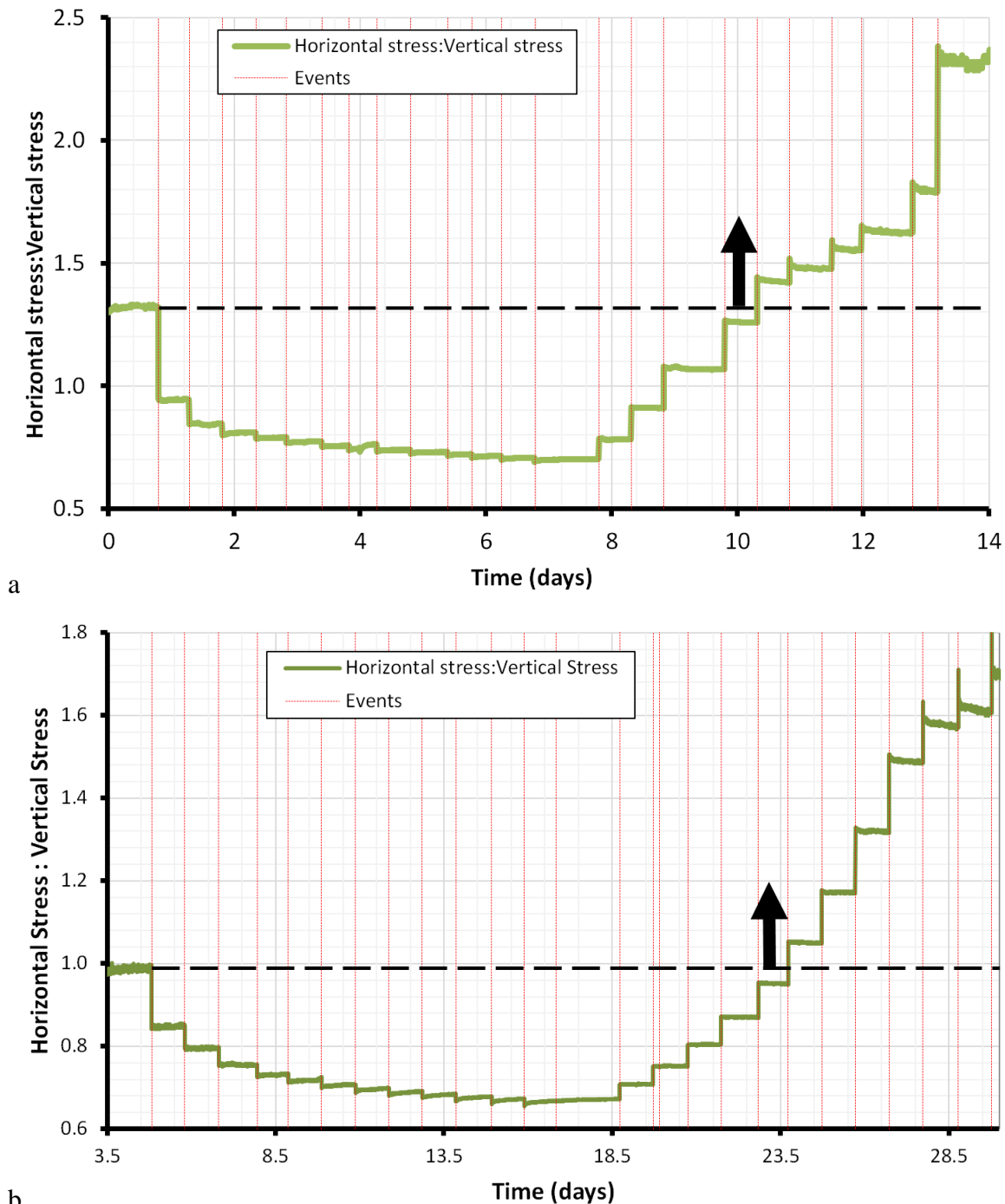


Figure 3-6 – The variation of the ratio of horizontal stress to vertical stress seen during loading-unloading experiments; a) water injection; b) gas injection. The arrows indicate horizontal stress to vertical stress ratios during unloading which are greater than the initial values and indicate an enhancement in flow rate.

Understanding the horizontal to vertical stress ratio is important in predicting the flow properties of discontinuities. Features experiencing high horizontal to vertical stress ratios are expected to be more conductive. High horizontal to vertical stress scenarios are likely to be more prevalent in regions experiencing stress relaxation due to structural uplift or removal of the overburden.

Again, this highlights that an understanding of the stress history of a discontinuity is essential to effectively predict the present fluid flow properties of those features.

3.1.4 Differences have been observed between injection fluids (water and helium), especially the hysteresis observed in flow. For water injection flow was only partially recovered during unloading, whereas for gas enhanced flow was seen at low normal loads.

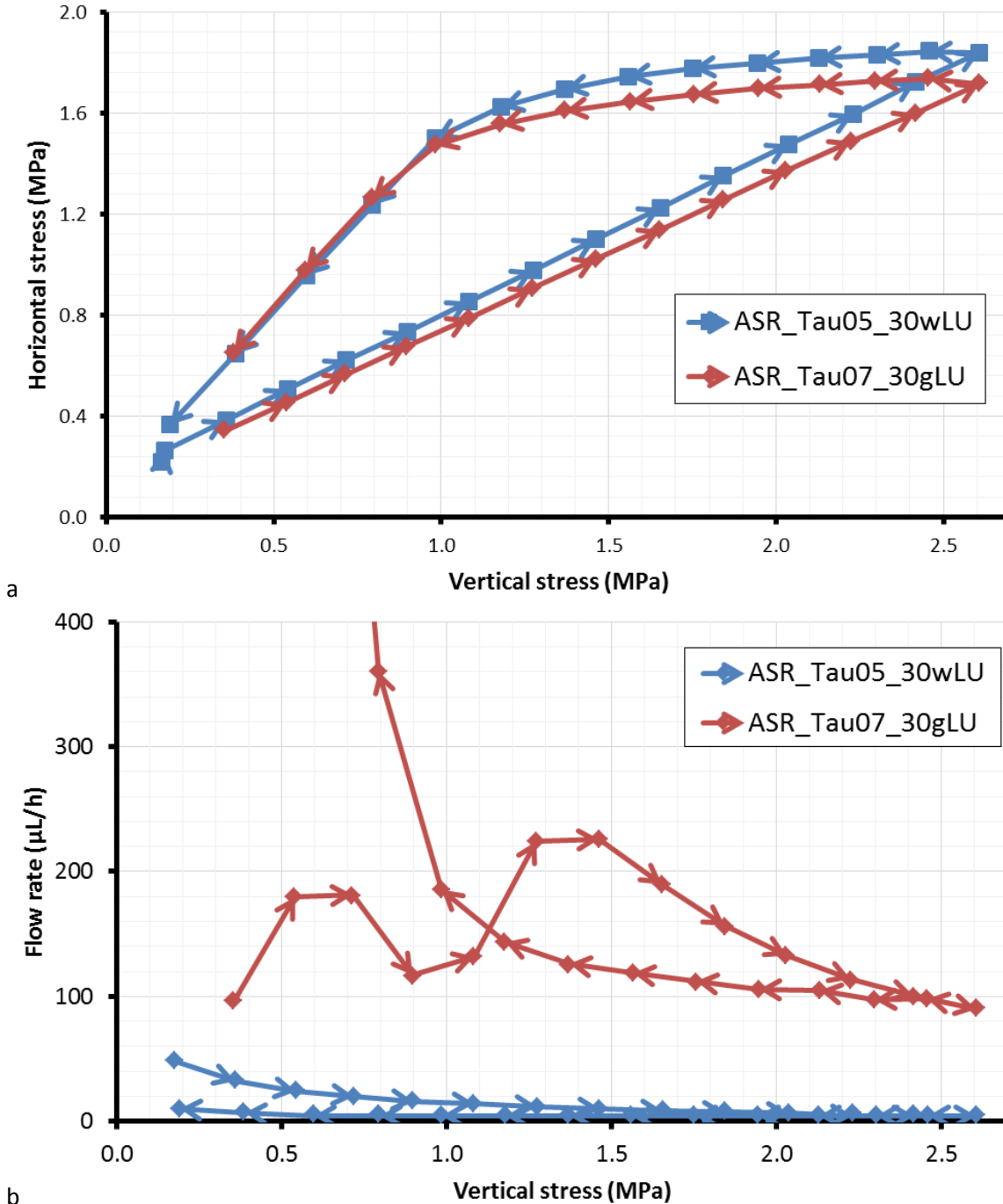


Figure 3-7 – Comparing results for water and gas injection during loading and unloading experiments; a) horizontal stress; b) flow response.

Figure 3-7a shows a comparison of the horizontal stress response during a loading-unloading experiment conducted using water and gas as the injection medium. There is agreement between the data recorded, which demonstrates that the gouge mechanically behaved the same way if water or gas was injected into a saturated kaolinite gouge. The similarities suggest that the gouge

was neither hydrated by water injection (as it is already fully saturated), nor was it desaturated by gas injection.

However, considerable differences were seen in flow behaviour. For water injection, a pore pressure of 1 MPa was sufficient to initiate flow, whereas a gas pressure in excess of 3.5 MPa was required. This resulted in much lower flow rates observed in water injection tests, as seen in Figure 3-7b. The differences suggest that the governing physics controlling gas movement is dissimilar to that controlling water movement.

As previously introduced, there was also considerable difference in the progression of flow during the loading cycle. At low vertical loads this behaviour was chaotic in gas injection, whereas it was smooth for water injection. By 1.5 MPa vertical load the two behaviours are similar, both decaying evenly with increasing vertical load.

Differences were also seen during the unloading cycle. Both injection fluids showed a similar initial response with considerable hysteresis seen and the slow recovery of flow. Dissimilarity was seen as vertical load reduced below approximately 1 MPa. For the case of water injection, flow was always only partially recovered. For gas injection, at low vertical loads flow increased to high levels much greater than that recorded at the corresponding vertical load on the loading cycle. The enhanced flow became catastrophic and at low vertical loads all gas in the gas reservoir was expelled through the slip-plane. Such catastrophic failure during water injection was not seen. This may in part be due to the expansion of gas as it propagated along the slip-plane as pressure reduced.

3.2 GAS BREAKTHROUGH EXPERIMENTS

A total of 26 gas breakthrough experiments were conducted on 0°, 15°, 30°, and 45° discontinuities; both with and without active shear. All tests were conducted in an identical manner with a known starting volume of 200 ml of helium at 4 MPa and a pressure ramp created by constant flow displacement of the ISCO syringe pump by 700 µl/h.

3.2.1 During gas breakthrough experiments episodic flow/fault valve behaviour was seen with a decrease in subsequent peak pressures and the form of the pressure response was different during subsequent breakthrough events.

A single test was conducted (ASR_Tau06) for a prolonged gas injection ramp to see if there was repeat gas entry. A total of seven steps were conducted, as seen in Figure 3-8. The exact detail of this particular test is complicated due to need to refill the gas reservoir several times and is described in detail in Cuss *et al.* (2013). However, general observations are introduced below.

It can be seen that the first gas breakthrough at 0.2 MPa vertical load resulted in the sudden catastrophic loss of gas pressure at 3.2 MPa as the gas reservoir was emptied through the slip-plane. Vertical load was increased to 1.85 MPa to see if a secondary breakthrough could be initiated following fracture sealing due to increased vertical load. This resulted in a distinct peak in gas pressure at 1.9 MPa, which was followed by a decay to 1.2 MPa and then slow recovery of gas pressure to another breakthrough at 1.6 MPa. Pressure dropped to 0.5 MPa and again recovered to another breakthrough event at about 1 MPa. This partial breakthrough was followed by pressure recovery to a plateau of 1.1 MPa. Vertical load was increased to 2.25 MPa and a fifth breakthrough occurred at 1.8 MPa.

The form of the breakthrough event changed during the experiment. The first event was a catastrophic total loss of pressure. The second event was a peak and trough, similar in form to that seen during gas injection in bentonite. The third event was a sudden drop in pressure by 1 MPa, and the fourth event could be described as the system reaching equilibrium and the attainment of a plateau.

These observations suggest that “fault-valve behaviour” had been demonstrated in the laboratory and the magnitude of subsequent break-through events reduced (at constant vertical load) and the

“form” of the breakthrough events changes with each successive feature. It also demonstrated that an increase in vertical load resulted in a degree of self-sealing, although the “memory” of previous breakthrough events may still be apparent.

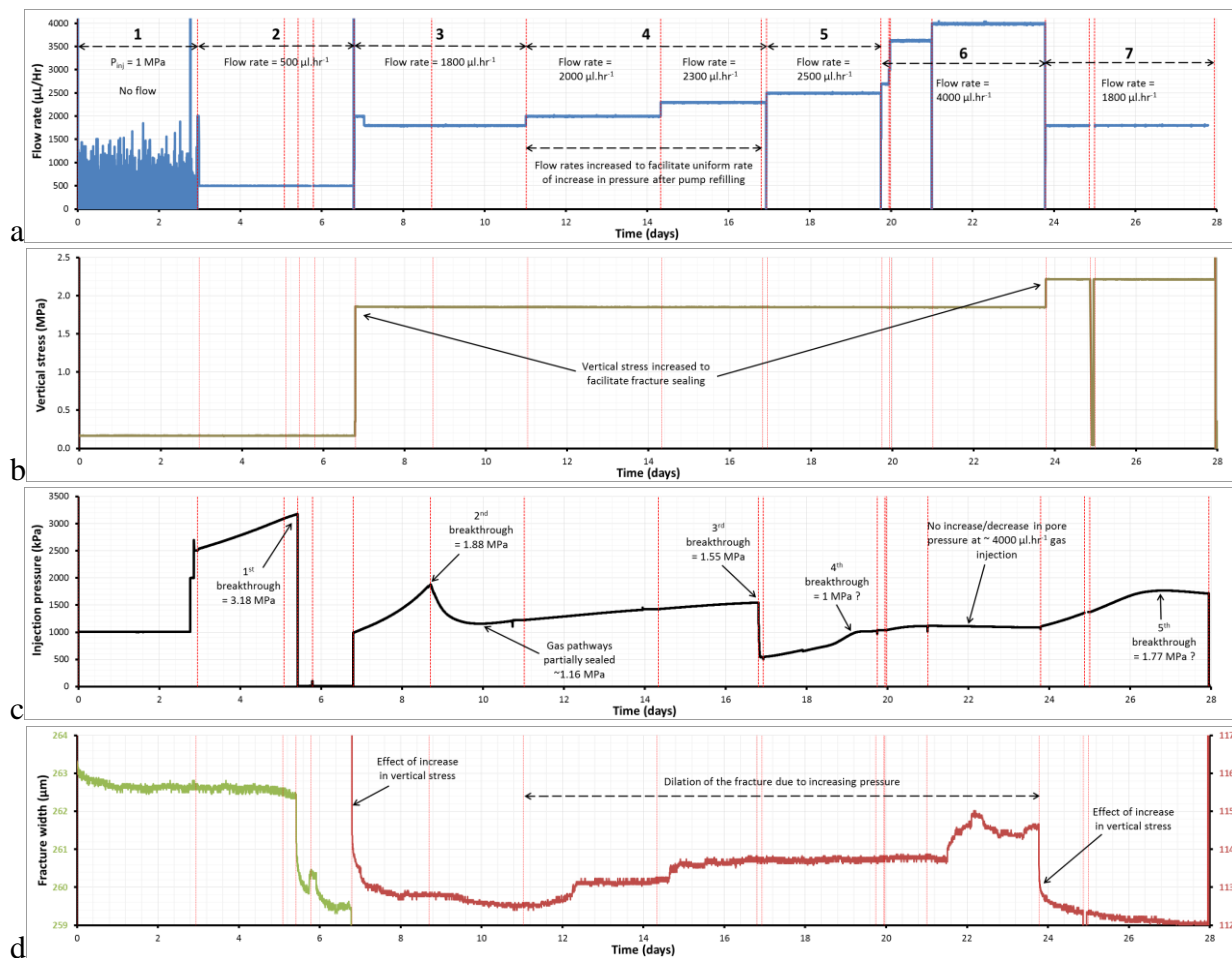


Figure 3-8 – Results from ASR_Tau06_30gGI showing different gas breakthrough indicating fault-valve behaviour. a) Flow rate versus time plot showing the gas injection rates used in different stages (indicated as numerals) of the experiment. b) Vertical stress versus time graph showing the vertical stresses applied on to the slip plane. c) Gas injection pressure versus time plot showing the evolution of injection pressure before and after each breakthrough event. d) The variations in fracture width during various gas injection stages.

3.2.2 Repeat gas injection testing has shown a consistent gas entry pressure but considerably different, non-repeatable, gas peak pressures.

Figure 3-9 shows an example of the repeatability of experimental results for four tests conducted on a discontinuity oriented at 30°. Gas entry pressure has been determined by comparing the gas pressure recorded with that predicted at the given pressure (Figure 3-9b). Three tests showed similar gas entry of approximately 8 MPa, with test ASR_Tau07 showing an anomalously low entry pressure of 5.5 MPa. This suggested that test ASR_Tau07 had gas entry at a much lower pressure for an unknown reason. Similar anomalously low gas entry pressures were seen on other orientations, suggesting that gas was able to exploit a “defect” of some form at a low pressure and the experiment was unable to be perfectly reproducible.

Whilst three of the four tests showed a similar gas entry pressure, these tests showed considerably different peak pressures of 10.8, 13.5, and 15.5 MPa (test ASR_Tau07 achieved a peak pressure of only 8.2 MPa). One test catastrophically broke-through at 10.8 MPa.

These observations suggest that the physical control on gas entry was repeatable, although in the presence of any form of imperfection gas was able to enter at lower pressures. Once gas started to move within the slip-plane the progression of pressure was less predictable and depended on whether the evolving gas network located an exit from the system. Similar results were seen for all discontinuity orientations.

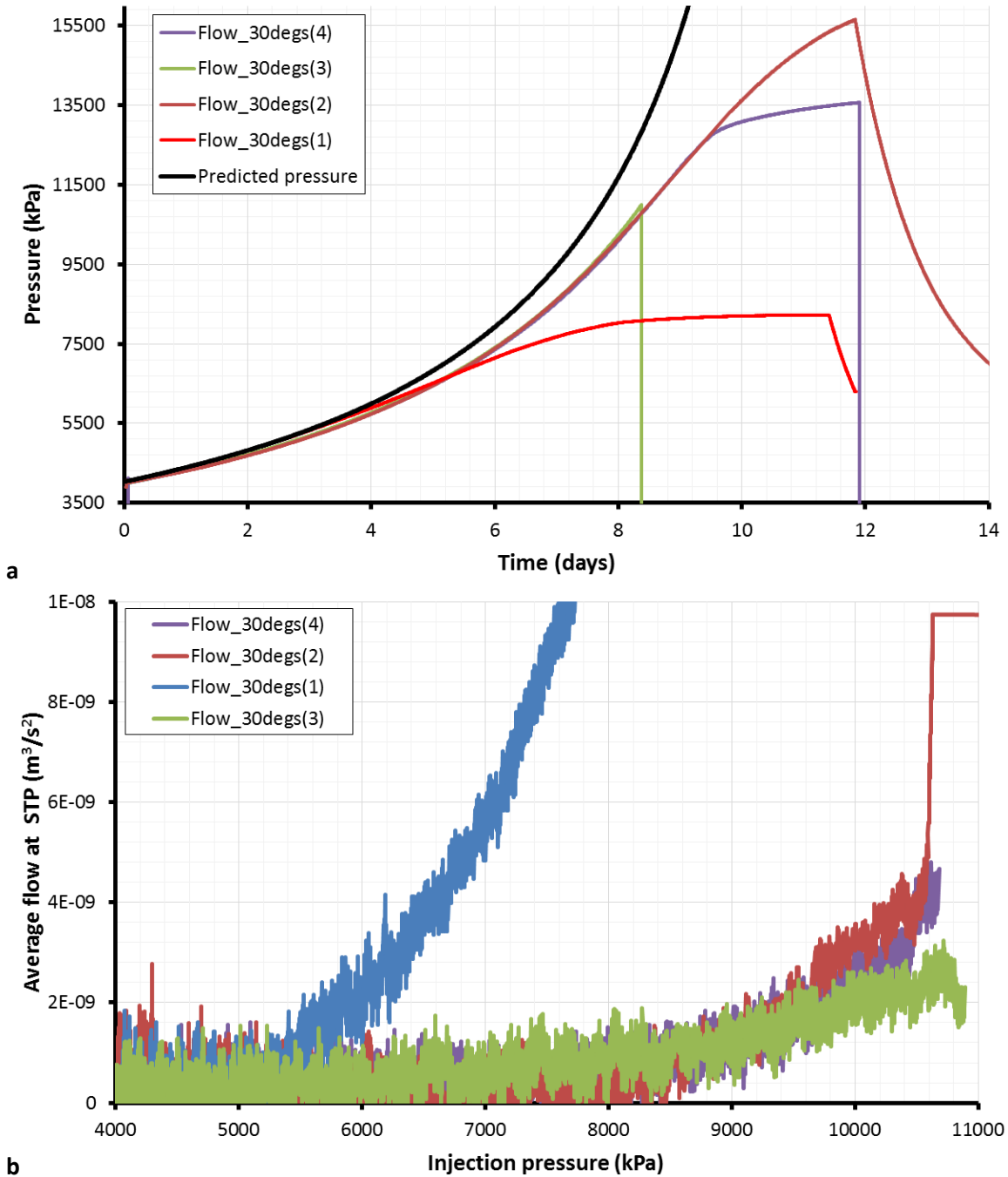


Figure 3-9 – Repeatability of gas injection tests; a) pressure response, b) flow results.

3.2.3 Differences in gas entry pressure are seen dependent on the orientation of the fracture.

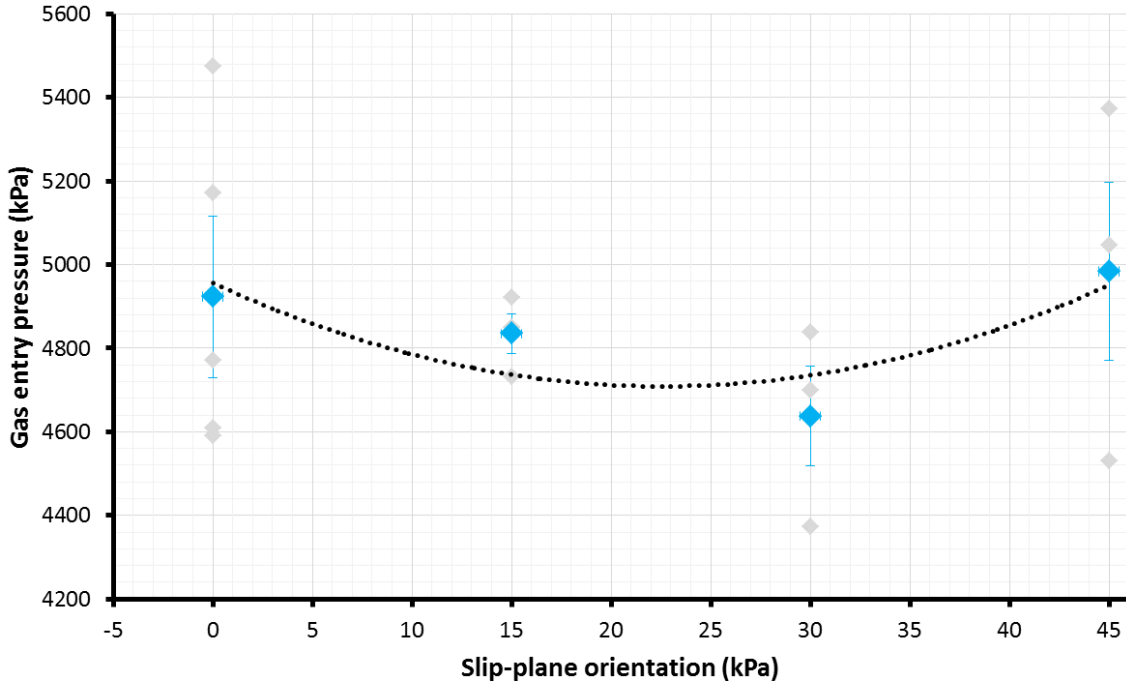


Figure 3-10 – Gas injection pressure variation with discontinuity orientation.

Although some tests have shown anomalously low gas entry pressures, Figure 3-10 shows a general variation of gas entry pressure with discontinuity orientation. The highest gas entry pressure, as expected, is seen on a flat slip-plane with an entry pressure of 8.5 MPa. The lowest gas entry pressure was recorded at 15° of 7.75 MPa. Generally, the results suggest that the lowest gas entry pressure would be observed at 22.5°.

All tests have been conducted at identical vertical loads. As discontinuity orientation varies, the load acting normal to the slip-plane will vary. Taking this geometrical effect into account, the variation seen in gas entry pressure is more complex than a simple stress rotation about the slip-plane, as shown in Figure 3-11.

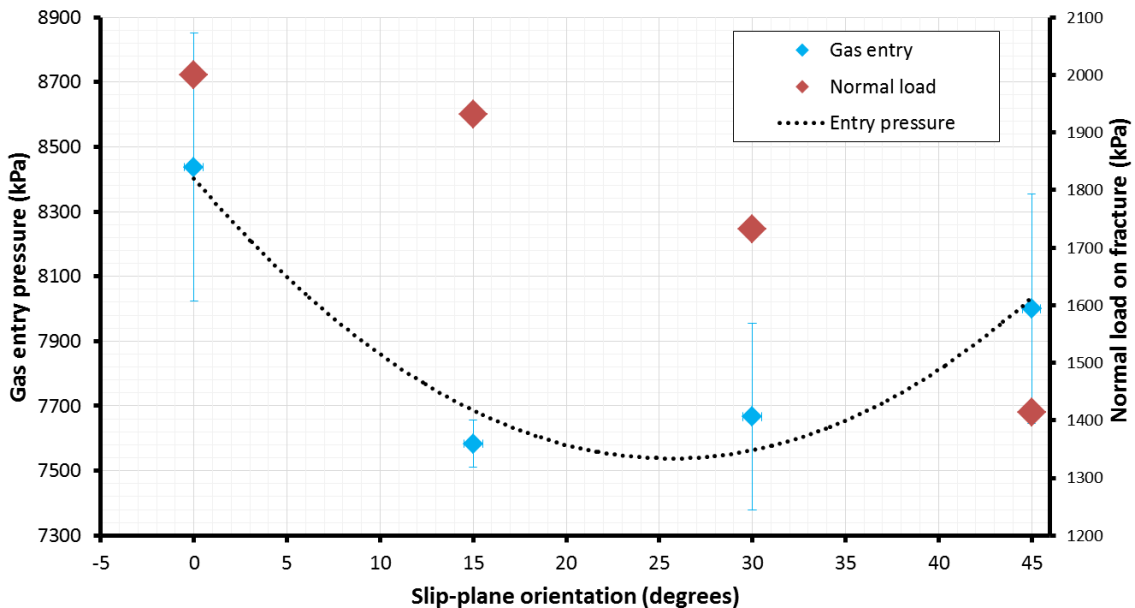


Figure 3-11 – Comparing gas entry pressure with normal load on the fracture.

The experimental study has clearly demonstrated a variation in fracture transmissivity with discontinuity orientation. This experimental study demonstrates that the critical stress theory is applicable in the absence of stress relaxation.

3.2.4 Active shear reduced the gas entry pressure; therefore in kaolinite shear has the opposite of self-sealing.

Figure 3-12 shows that tests conducted on slip-planes oriented to the direction of active shear showed a lower gas entry pressure for kaolinite and a rotation of gas entry pressure minimum to 38°. For water injection fracture transmissivity was seen to reduce due to self-sealing as a result of shearing. Therefore the reduction in gas entry pressure and observed increase in flow (as postulated from a reduced peak pressure) suggests that shearing in kaolinite has the opposite effect of self-sealing to gas.

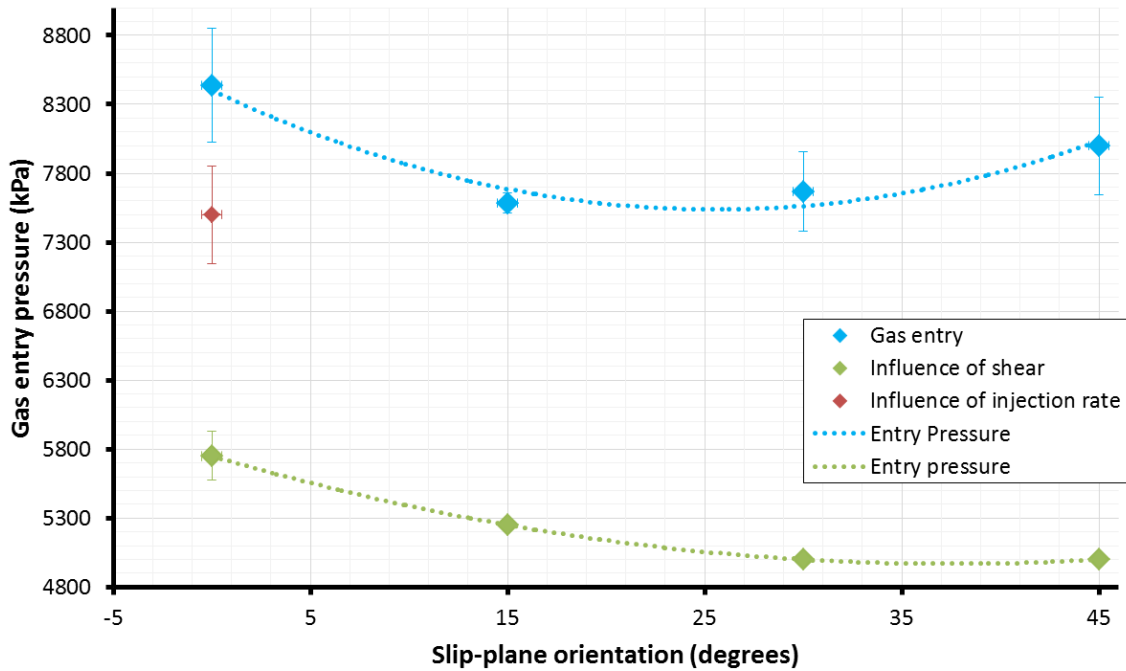


Figure 3-12 – Gas injection pressure variation with discontinuity orientation and the influence of shear and injection rate.

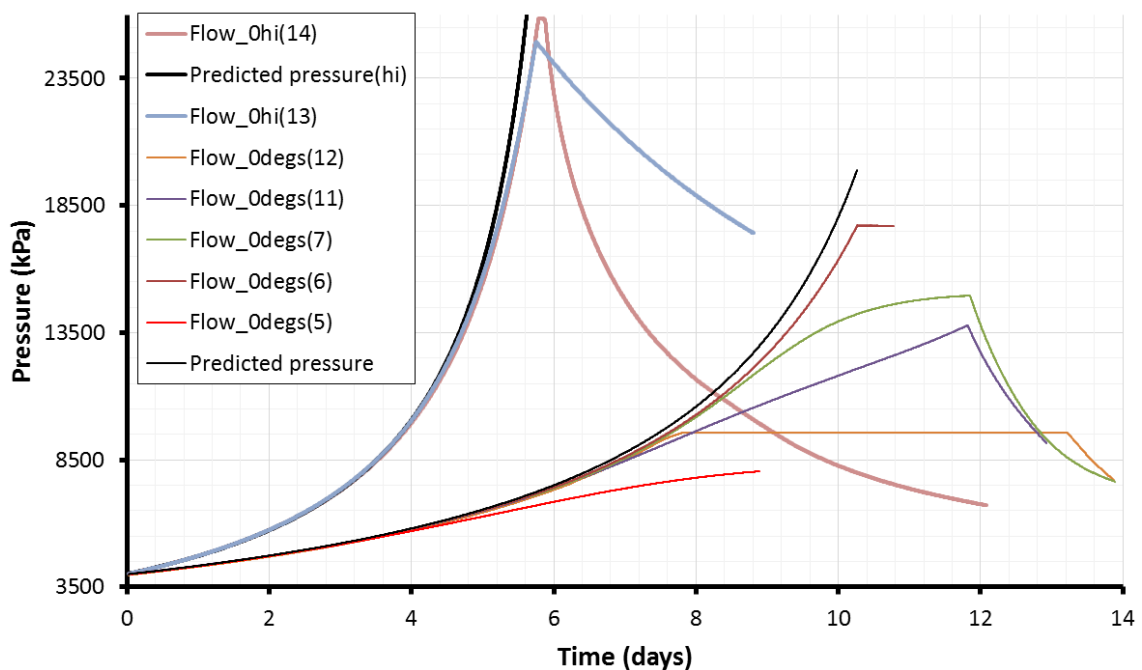


Figure 3-13 – The influence of gas pressurisation rate.

3.2.5 The response of the kaolinite gouge was rate dependent, with a change in entry pressure and peak pressure response.

Figure 3-12 and Figure 3-13 show that the test results were rate dependent. Two tests were conducted with an increased gas injection rate and both tests showed similar general results. An increased gas injection rate significantly altered the gas response of the gouge (Figure 3-13); with significantly higher gas pressure achieved in excess of 24 MPa. Neither test showed signs of reaching peak pressure behaviour.

Both tests had similar gas entry pressure when determined from STP flow, which was marginally lower than the gas entry pressure for all other tests conducted (Figure 3-12). This suggested that the rate of pressurisation had only a small effect on gas entry, but once gas was mobile within the kaolinite gouge it had a significant influence.

3.3 GENERAL OBSERVATIONS

3.3.1 The results showed that the flow of fluids through clay filled fractures was non-uniform and occurred via localised preferential pathways.

Three tests were conducted and recorded using time-lapse photography to observe the escape of gas from the slip-plane into the bath of the apparatus.

All three of these experiments showed that a small, isolated stream of bubbles escaped from a single location. In all tests a single stream of bubble was created, i.e. a single pathway and a second pathway either had not formed or did not reach the edge of the slip-plane. However, one test showed two exit points from the gouge and evidence of pathway evolution once gas was able to escape. In all tests the frequency of escaping bubbles increased, as did their size.

Fracture width data were inconsistent in recording dilation events at the onset of gas flow. However, some tests clearly showed dilation. This observation combined with the isolated single bubble stream show that gas propagated by means of a dilatant process.

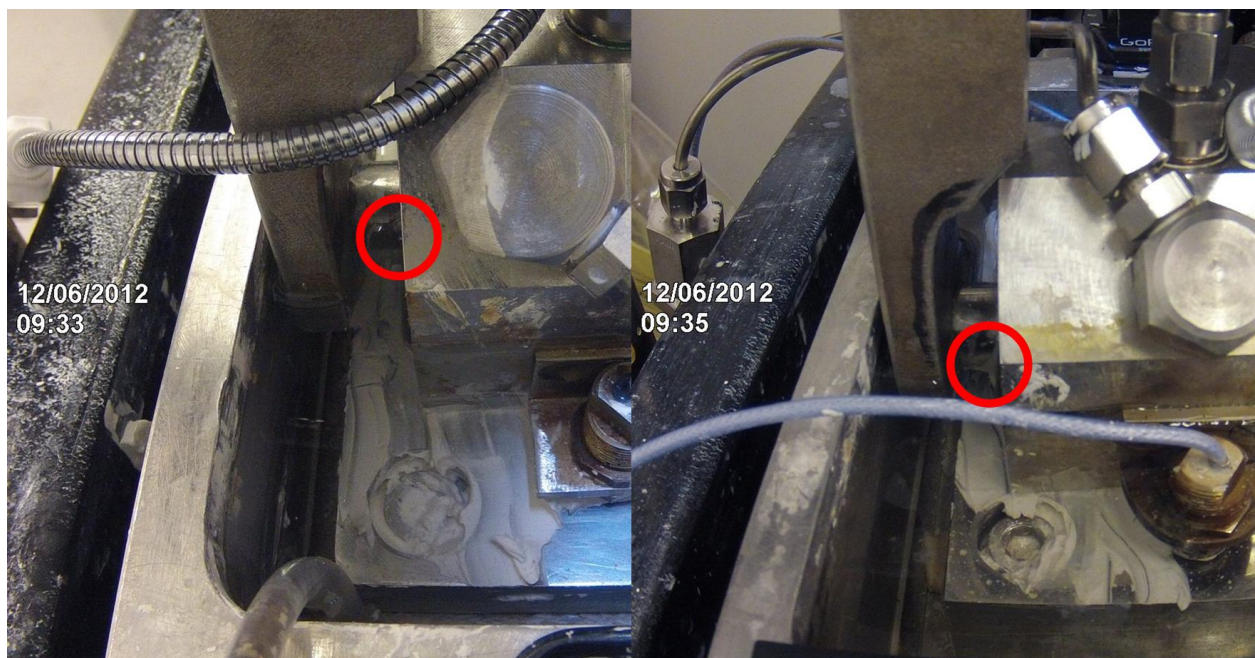


Figure 3-14 – Photo showing the escape of gas into from the slip-plane.

3.3.2 The pressure recorded within the slip-plane showed a negligible fracture pressure and did not vary much in all tests.

In all tests, the two pressure ports located within the slip-plane registered pressure less than 50 kPa, effectively close to zero (see Figure 3-15). Little variation was seen, although some changes

occurred during loading-unloading experiments as a result of consolidation. However, no evidence of elevated gas pressures were seen during any experiment. This strengthens the observation of localised dilatant pathways as opposed to a distributed radial migration of gas.

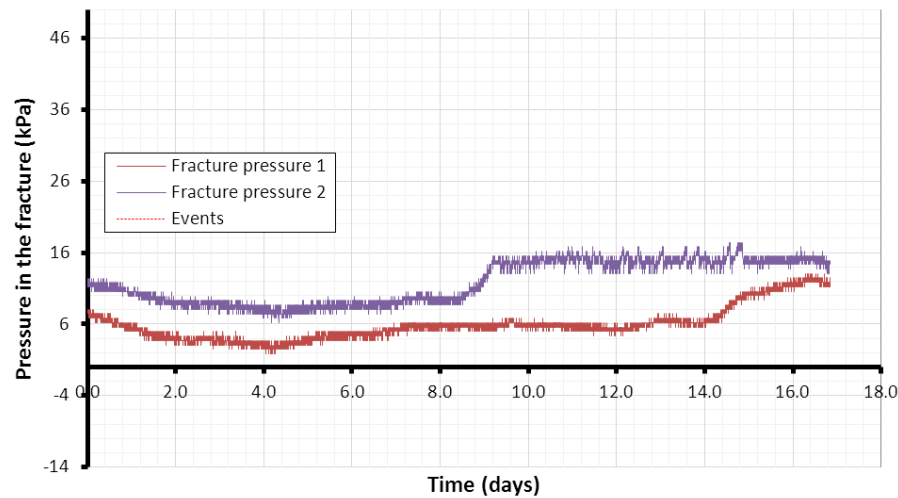


Figure 3-15 – Example of pressure recorded on the slip-plane. A low pressure of less than 20 kPa is observed. Little variation is seen, with no correlation with other data identified. Compare this data with the gas injection pressure seen in Figure 3-14.

4 Conclusions

This report describes an experimental study of 48 separate experiments with the primary aim to verify critical stress theory. Two main types of experiment were conducted: 1). Loading-unloading tests, where fracture flow was monitored at constant injection pressure as normal load was increased in steps to a given level and then reduced back to the starting stress state; 2). Gas breakthrough experiments, where gas injection pressure was increased in a pressure ramp at constant vertical load. These were conducted with and without active shear. It was found that critical stress theory is valid in predicting the preferential flow of gas in relation to the orientation of the fracture plane with respect to the maximum horizontal stress direction. However, loading unloading experiments showed that understanding the stress history of the rocks is of paramount importance and a mere knowledge of the current stress state is insufficient in accurately predicting the nature of fluid flow.

A total of 17 loading-unloading experiments were conducted, all on a 30° slip-plane. The main conclusions of this part of the study were; a). During a loading (vertical stress) and unloading cycle considerable hysteresis in flow was observed signifying the importance of stress history on fracture flow; b). For the case of gas injection the change in flow is chaotic at low normal loads, whereas for water injection the flow reduces smoothly with increased normal load; c). Hysteresis in horizontal stress observed during unloading demonstrates the importance of the ratio between horizontal stress and vertical stress and its control on flow; d). Differences have been observed between injection fluids (water and helium), especially the hysteresis observed in flow. For water injection flow is only partially recovered during unloading, whereas for gas enhanced flow is seen at low normal loads.

A total of 26 gas breakthrough experiments were conducted on 0°, 15°, 30°, and 45° discontinuities; both with and without active shear. All tests were conducted in an identical manner. The main conclusions of this part of the study were; a). During gas breakthrough experiments episodic flow/fault valve behaviour was seen with a decrease in subsequent peak pressures and the form of the pressure response was different during subsequent breakthrough events; b). Repeat gas injection testing had shown a consistent gas entry pressure but

considerably different, non-repeatable, gas peak pressures; c). Differences in gas entry pressure were seen dependent on the orientation of the fracture; d). Shear can be seen to reduce the gas entry pressure, suggesting that shearing in kaolinite has the opposite effect of self-sealing to gas.

Other general observations of gas flow along fractures included; a). The flow of fluids through clay filled fractures is non-uniform and occurs via localised preferential pathways; b). The pressure recorded within the slip-plane showed a negligible fracture pressure and did not vary much in all tests.

References

British Geological Survey holds most of the references listed below, and copies may be obtained via the library service subject to copyright legislation (contact libuser@bgs.ac.uk for details). The library catalogue is available at: <http://geolib.bgs.ac.uk>.

- Barton, C. A., Zoback, M. D., and Moos, D. (1995) Fluid flow along potentially active faults in crystalline rock. *Geology*, **23**, no. 8, pp. 683-686.
- Bossart, P., Meier, P. M., Moeri, A., Trick, T., and Mayor, J.-C. (2002) Geological and hydraulic characterisation of the excavation disturbed zone in the Opalinus Clay of the Mont Terri Rock Laboratory. *Engineering Geology*, **66**, no. 1-2, p. 19-38.
- Brudy, M., Zoback, M. D., Fuchs, K., Rummel, F., and Baumgärtner, J. (1997) Estimation of the complete stress tensor to 8 km depth in the KTB scientific drill holes: Implications for crustal strength. *Journal of Geophysical Research-Solid Earth*, **102**, no. B8, p. 18453-18475.
- Cuss, R.J., Sathar, S., and Harrington, J.F. (2013) Validation of critical stress theory applied to repository concepts. *British Geological Survey Commissioned Report*, **CR/13/001**. 1059pp.
- Cuss, R.J., Milodowski, A., and Harrington, J.F. (2011) Fracture transmissivity as a function of normal and shear stress: first results in Opalinus clay. *Physics and Chemistry of the Earth*. **36**, pp.1960-1971.
- Cuss, R.J., Sathar, S., and Harrington, J.F. (2012) Fracture transmissivity test in Opalinus Clay. *British Geological Survey Commissioned Report*, **CR/12/132**. 63pp.
- Finkbeiner, T., Barton, C. A., and Zoback, M. D. (1997) Relationships Among In-Situ Stress, Fractures and Faults, and Fluid Flow, Monterey, Formation, Santa Maria Basin, California. *AAPG Bulletin*, **81**, p. 1975-1999.
- Heffer, K., and Lean, J. (1993) Earth stress orientation - a control on, and guide to, flooding directionality in a majority of reservoirs, Tulsa, PennWell Books, *Reservoir Characterization III*, 799-822 p.:
- Jaeger, J. C., Cook, N. G. W., and Zimmerman, R. W. (2007) *Fundamentals of rock mechanics*, Wiley-Blackwell.
- Laubach, S. E., Olson, J. E., and Gale, J. F. W. (2004) Are open fractures necessarily aligned with maximum horizontal stress? *Earth and Planetary Science Letters*, **222**, no. 1, p. 191-195.
- Reeves, H. (2002) *The effect of stress and fractures on fluid flow in crystalline rocks*, Cumbria, PhD Thesis, University of Durham, 239 p.
- Rogers, S. F. (2003) Critical stress-related permeability in fractured rocks. *Fracture and in-Situ Stress Characterization of Hydrocarbon Reservoirs*, **209**, p. 7-16.
- Rogers, S. F., and Evans, C. J. (2002) Stress-dependent Flow in Fractured Rocks at Sellafield, United Kingdom. *AAPG Special Volumes, v. AAPG Methods in Exploration No. 13: Geological Applications of Well Logs*, p. 241-250.
- Rutqvist, J., Børgesson, L., Chijimatsu, M., Hernelind, J., Jing, L., Kobayashi, A., and Nguyen, S. (2009) Modeling of damage, permeability changes and pressure responses during excavation of the TSX tunnel in granitic rock at URL, Canada. *Environmental Geology*, **57**, no. 6, p. 1263-1274.

- Sathar, S., Reeves, H.J., Cuss, R.J., and Harrington, H.J. (2012) Critical stress theory applied to repository concepts; the importance of stress tensor and stress history in fracture flow. *Mineralogical Magazine*.
- Zoback, M. D., Moos, D., Mastin, L., and Anderson, R. N. (1985) Well bore breakouts and in situ stress. *Journal of Geophysical Research-Solid Earth*, **90**(B7), p. 5523-5530.